
Value-Consistent Representation Learning for Data-Efficient Reinforcement Learning

Yang Yue^{1,2*} Bingyi Kang¹ † Zhongwen Xu¹ Gao Huang² Shuicheng Yan¹

¹Sea AI Lab ²Department of Automation, BNRist, Tsinghua University
{yueyang, kangby, xuzw, yansc}@sea.com, gaohuang@tsinghua.edu.cn

Abstract

Deep reinforcement learning (RL) algorithms suffer severe performance degradation when the interaction data is scarce, which limits their real-world application. Recently, visual representation learning has been shown to be effective and promising for boosting sample efficiency in RL. These methods usually rely on contrastive learning and data augmentation to train a transition model for *state* prediction, which is different from how the model is used in RL—performing *value*-based planning. Accordingly, the learned model may not be able to align well with the environment and generate consistent value predictions, especially when the state transition is not deterministic. To address this issue, we propose a novel method, called *value-consistent representation learning* (VCR), to learn representations that are directly related to decision-making. More specifically, VCR trains a model to predict the future state (also referred to as the “imagined state”) based on the current one and a sequence of actions. Instead of aligning this imagined state with a real state returned by the environment, VCR applies a Q -value head on both states and obtains two distributions of action values. Then a distance is computed and minimized to force the imagined state to produce a similar action value prediction as that by the real state. We develop two implementations of the above idea for the discrete and continuous action spaces respectively. We conduct experiments on Atari 100K and DeepMind Control Suite benchmarks to validate their effectiveness for improving sample efficiency. It has been demonstrated that our methods achieve new state-of-the-art performance for search-free RL algorithms.

1 Introduction

An important research direction in Deep Reinforcement Learning (RL) is to improve data efficiency, which is much demanded by the wide application of deep RL techniques in real-world scenarios. With the state-of-the-art RL algorithms, simple tasks such as Atari Learning Environment [4] games require billions of frames (or equivalently 10-50 years of human experiences) to achieve human-level performance [2]. In real-world applications, such as robot controllers and self-driving systems, it is impractical to obtain such a huge amount of interaction due to the costly data collection process. To enable deep RL to go beyond virtual games and simulators, researchers explore the data efficiency issue from various perspectives, including model-based RL [16, 15, 22], auxiliary tasks [20, 41], self-supervised training for representation [25, 28, 33, 44, 29], etc. A majority of the works borrow ideas from the wider deep learning community to create additional training signals thus accelerating the agent training process. Most of these techniques are not specifically tailored for RL problems and some heavily rely on image inputs and augmentations.

*This work was done when Yang Yue was an intern at Sea AI Lab.

†Corresponding Author.

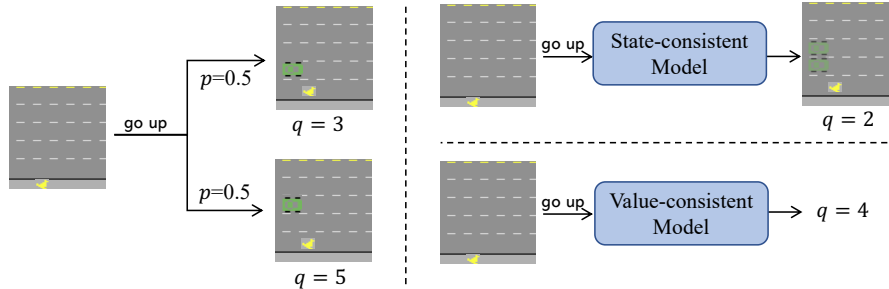


Figure 1: **Left:** A stochastic environment where the agent needs to navigate up to cross the road while avoiding collision with cars. When the agent takes the action “go up”, a car randomly appears from two different positions with equal probabilities, resulting in different trajectory returns (e.g., 3 v.s. 5). **Right top:** A state-consistent model is usually trained to produce state predictions that are consistent with the ground truth. It will generate a “mixed” state in this situation, based on which a value network may give arbitrary value estimations (e.g., 2). **Right bottom:** A value-consistent model is learned by aligning the values of its imagined state and the corresponding real state. In the stochastic setting, it can make a correct prediction of the expected return, as the supervision conducted at training.

Recently, Self-Predictive Representations (SPR) [33] introduces contrastive learning into transition model learning and boosts the performance of RL in a low-data regime significantly. More specifically, SPR aims at learning an embedding space in which the agent can predict future state embeddings that are indistinguishable from the real states. Despite its effectiveness, it solely focuses on learning discriminative state features, ignoring the fact that some information in the raw observations is unnecessary or even distracting for decision-making. Moreover, it is possible in practice that two states result in significantly different returns while being visually similar. Kielak [39] and van Hasselt *et al.* [23] also argue that training a transition model without planning purpose is unlikely to address the data inefficiency issue. For example, as shown in Fig. 1, when the environment dynamics is stochastic, it would be difficult for the learned model to make a correct state prediction, resulting in arbitrary value estimations. Instead, a model learned directly with trajectory returns can produce an expected return from the current state-action pair, which is exactly how the Q -value is defined and updated with Bellman Equation.

Similar observations have been made on the Value Equivalence (VE) principle [13] for model-based RL, which advocates that a model should be able to generate the same updates as the real environment under corresponding Bellman operators, rather than directly modeling state-to-state transitions. The success of some state-of-the-art algorithms such as MuZero [32], Value Prediction Network [31] and Predictron [35] can be attributed to this principle. However, value equivalence is only studied with state value functions $V(S)$, and is often coupled with policy-based algorithms, which makes it non-trivial to apply VE for value-based RL.

In this paper, we develop a value-consistent metric for action-values (*i.e.*, Q -values) and propose a novel method called *Value-Consistent Representation Learning* (VCR) to boost sample efficiency for action-value based RL methods. In contrast to existing data-efficient RL ideas, VCR is based on RL semantics other than losses constructed purely upon input states. Specifically, we introduce a dynamics model to predict the next states in a latent representation space induced by a state encoder. When a real trajectory from the environment is provided, our dynamics model can roll out an imagined trajectory from the initial state by taking the same sequence of actions. Then, for each of the real and imagined state pairs, we obtain two Q -value distributions (over all available actions). A value-consistent loss function is applied to align these two distributions. VCR can be viewed as a clean implementation of value equivalence with action-values so that it is highly extendable in a significant family of RL algorithms. The idea is simple yet effective and it can be easily integrated into any value-based RL algorithm. We demonstrate the effectiveness of the idea with two concrete implementations based on Rainbow DQN [19] and Soft Actor-Critic (SAC) [14], covering environments with both discrete and continuous actions.

We conduct extensive experiments to validate the effectiveness of VCR on two benchmarks: Atari 100K [4, 22] (discrete action) and DeepMind Control Suite [38] (continuous action). Despite its simplicity, the results clearly show our method can boost sample efficiency significantly and achieve

new state-of-the-art. Our method surpasses SPR on Atari 100K by 6 absolute points in terms of the human-normalized score, on DeepMind Control Suite by 40 scores.

2 Related Work

2.1 Data-Efficient Reinforcement Learning

Reinforcement learning algorithms suffer severe performance degradation when only a limited number of interactions are available. There are various methods trying to tackle this problem, by either model-based [22] or model-free learning [39, 23, 40, 25]. For example, SimPLe [22] utilizes a world model learned with collected data to generate imagined trajectories, which are combined with real trajectories to train the agent. Experiments on the Atari 100K benchmark [22] demonstrate its superiority for boosting sample efficiency. Later, Data-Efficient Rainbow [39] and OTRainbow [23] show that Rainbow DQN [19] with hyperparameter tuning can be a strong baseline for the low-data regime by simply increasing the number of steps in multi-step return and allowing more frequent parameter update.

Recently, leveraging computer vision techniques is drawing increasingly more attention from the community to boost representation learning in RL [40, 26, 41, 25, 33, 29, 43, 44, 42]. DrQ [40] makes a successful attempt by introducing image augmentation into RL tasks where an agent takes visual inputs, while Yarats *et al.* [41] use image reconstruction as an auxiliary loss function. Inspired by the remarkable success of contrastive learning for representation learning [17, 6, 12, 7], the contrastive loss has been integrated into RL as an effective component [25, 33, 29, 43, 44, 25, 42]. For example, CURL [25] forces different augmentations of the same state to produce similar embeddings and different states to generate dissimilar embeddings, with the contrastive loss [17] jointly optimized with an RL loss.

More recently, SPR [33] and KSL [29] make a more sophisticated design by employing contrastive loss in transition model learning. In this way, an agent can learn representations that are predictable when the previous state and action are given, thus boosting the performance significantly. As a follow-up, PlayVirtual [44] introduces a backward prediction model that enables the agent to imagine forward and backward to form a cycle. Therefore, arbitrary actions instead of the actual ones can be taken in imagination and a cycle-consistent loss function can be used for supervision. EfficientZero [42] introduces the self-predictive loss in SPR into MuZero [32], achieving super-human performance on the Atari 100K benchmark for the first time.

These successes demonstrate that self-predictive representation learning is indeed a promising way to improve sample efficiency. We also choose to base our method on SPR. However, these methods only focus on making accurate state predictions, ignoring the fact that value prediction is key to decision making. In this work, we propose value-consistent representation learning and show it is important for making a better decision.

2.2 Value Equivalence Principle

Some works in model-based RL have proposed a high-level idea of learning the transition model in terms of the value space [9, 8, 13, 31, 37, 32, 18, 5]. Value-Aware Model Learning (VAML) [9, 8] incorporates the knowledge of value function into optimization to learn the probabilistic transition model in model-based reinforcement learning. Grimm *et al.* [13] come up with the value equivalence principle which forces the learned transition model to have the same Bellman operator updates with the real environment model conditioned on a set of value functions and policies. Several empirically successful works like VPN [31], VIN [37] and MuZero [32] can be viewed as the instances that follow the value equivalence principle when considering diverse forms of Bellman operators and value approximations. Self-consistent models and values [10] boosts the performance of Muesli agent [18] by encouraging a value function to satisfy the Bellman equation under a learned transition model and a learned policy.

Although based on similar motivation as the value equivalence principle, our core idea greatly differs from the above works. Almost all above works lie in the category of planning-based RL and leverage value regularization or value equivalence to train a better parameterized dynamics model for planning. However, our method, closer to model-free algorithms, harnesses value consistency to learn a transition model for better state representation. Additionally, our method employs the reward

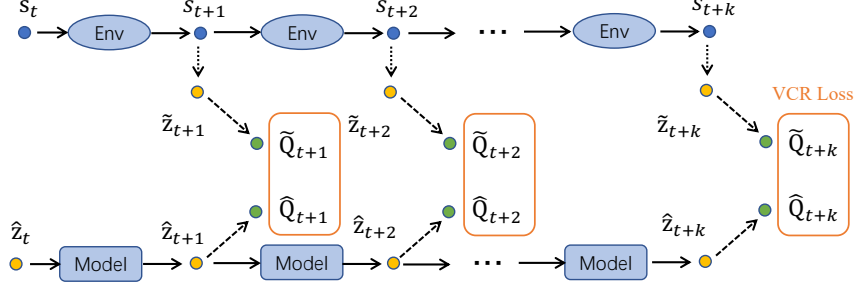


Figure 2: **Pipeline of Value-Consistent Representation Learning.** Blue, yellow, and green dots denote states from the environment, latent states in embedding space, and q value distributions respectively; orange boxes denote the distance metric. The agent interacts with the environment to produce a sequence of states $\{s_{t+k}\}_{k=1:K}$. The sequence is encoded into a latent embedding space, denoted as $\{\tilde{z}_{t+k}\}_{k=1:K}$. Then the parametric transition model predicts the sequence of latent states $\{\hat{z}_{t+k}\}_{k=1:K}$ conditioned on the start point \hat{z}_t and the action sequence, where \hat{z}_t is the latent embedding from s_t . Instead of aligning the predictions in the latent embedding space, Value-Consistent Representation Learning enforces the value prediction from imagined states to be consistent with the values of a real state from the environment. For simplicity, action inputs to the environment and the transition model are omitted.

from the real environment to estimate the target value, while those planning algorithms use predicted rewards and need a reward prediction model.

3 Method

We are especially interested in Reinforcement Learning (RL) in a low-data regime, where only a limited number of interactions are allowed. In this section, we detail our value-consistent representation (VCR) learning method step by step. First, we prepare the readers with certain preliminaries required by VCR. Then, we introduce the intuition and the overall framework for VCR. In the end, we provide two implementations of VCR for both discrete and continuous action settings.

3.1 Preliminaries: Value-Based Reinforcement Learning

Reinforcement Learning (RL) addresses the problem of sequential decision making, which is usually formulated with a Markov Decision Process (MDP). A typical MDP is represented with a tuple $\langle \mathcal{S}, \mathcal{A}, T, r, \gamma \rangle$. Here \mathcal{S} is a finite set of states; \mathcal{A} is the action space; $T(s, a, s') = P(s'|s, a)$ is the dynamics function describing the probability of transitioning from a state s to s' after taking an action a ; $r(s, a, s')$ and $\gamma \in (0, 1]$ are the reward function and the discount factor respectively. An agent interacts with an MDP environment by repeatedly taking action a_t at s_t , and receives a reward r_{t+1} . Then the environment transits to the next state s_{t+1} . The fundamental goal of RL is to learn an agent maximizing the discounted cumulative reward (*i.e.*, return) $G_t = \sum_{\tau=0}^{\infty} \gamma^\tau r_{t+\tau+1}$ at any time step t . The behavior of an agent is denoted by a policy $\pi(a|s)$ mapping from states to actions, while the action-value function $Q_\pi(s, a) = \mathbb{E}_\pi [G_t | s_t = s, a_t = a]$ predicts the expected return if the agent takes an action a for state s at the time step t , following the policy π .

There are various ways to learn the optimal policy π^* . In this paper, we focus on value-based RL algorithms that are rooted in Q -learning. Q -learning performs approximate dynamic programming by following the Bellman equation [36]. It first randomly initializes all Q values and then repeatedly updates them according to the update rule $Q(s, a) \leftarrow Q(s, a) + \alpha [r + \gamma \max_{a'} Q(s', a') - Q(s, a)]$, where $\alpha \in (0, 1]$ is a learning rate. Deep Q Network (DQN) [30] scales Q -learning to large state (*e.g.*, visual inputs) and action spaces by utilizing neural networks to encode states and generate Q values. Additionally, experience replay and a separated target network are used to stabilize the training of DQN. The overall objective for DQN is given by

$$\mathcal{J}(\theta) = \mathbb{E}_{(s, a, s', r) \sim \mathcal{D}} \left[\left(r + \gamma \max_{a'} Q_{\bar{\theta}}(s', a') - Q_{\theta}(s, a) \right)^2 \right], \quad (1)$$

where Q_θ is the Q network parameterized with θ , $Q_{\bar{\theta}}$ is the target Q network, and \mathcal{D} represents the replay buffer which stores the experience tuples. Let $\bar{G}_t^{(n)} = \sum_{\tau=1}^n \gamma^{\tau-1} r_{t+\tau} + \gamma^n \max_a Q_{\bar{\theta}}(s_{t+n}, a)$ be the n -step value target. Note that when $n = 1$, it reduces to the estimator used in Eqn. (1), but $n > 1$ is also commonly used to get a better estimation [36, 19].

As the main goal of our work is to boost the sample efficiency of RL algorithms, without loss of generality, we build our method upon two best-performing algorithm variants, *i.e.*, Rainbow DQN [19] for discrete action domains and Soft Actor-Critic (SAC) [14] for continuous action domains. Rainbow DQN utilizes a distributional representation [3] for Q values by discretizing them into multiple bins, making the loss function slightly different from Eqn. (1). Also, SAC makes certain modifications to make it applicable to continuous actions. For more details, please refer to Appendix A.1 or their papers. Though empirical results are only shown with these two algorithms, our method is general enough to be easily integrated into any other value-based RL algorithms.

3.2 Value-Consistent Representation Learning

Various methods have shown that representation learning can boost the sample efficiency of RL. However, all these methods approach the problem from a computer vision perspective, *i.e.*, encouraging similar states to generate similar embeddings and forcing different states to be discriminative. Despite their effectiveness, visual recognition is not always directly related to decision-making. To alleviate this issue, we base our method on the assumption [33, 44, 42] that an agent should be able to predict the resulting state following a sequence of actions. Instead of aligning the predictions in the embedding space, our key idea is the value prediction from an *imagined state* should be consistent with the values of a *real state* from the environment, as illustrated in Fig. 2. Thus, the method is termed Value-Consistent Representation Learning (VCR).

State Prediction with Transition Model. Considering a one-step interaction between an agent and the environment: (s_t, a_t, s_{t+1}) , s_{t+1} can be determined by the transition T in the underlying MDP, given (s_t, a_t) . Similar to SPR [33] and PlayVirtual [44], we introduce a parametric transition model $h(\cdot, \cdot)$ to mimic the behavior of T in a latent embedding space. More specifically, a (convolutional) neural encoder $f(\cdot)$ is used to encode a pixel-based observation/state s_t into a latent representation $z_t = f(s_t)$. Then $h(\cdot, \cdot)$ operates by $\hat{z}_{t+1} = h(z_t, a_t)$. As shown in Fig. 2, based on the current latent state z_t , following a sequence of future K actions $a_{t:t+K-1}$, a sequence of state predictions $\hat{z}_{t+1:t+K}$ is obtained by applying $h(\cdot, \cdot)$ recursively:

$$\begin{aligned} \hat{z}_t &= z_t = f(s_t) \\ \hat{z}_{t+k+1} &= h(\hat{z}_{t+k}, a_{t+k}), \quad k = 0, 1, \dots, K-1. \end{aligned} \quad (2)$$

The transition model $h(\cdot, \cdot)$ is usually optimized to minimize the prediction error between $\hat{z}_{t+1:t+K}$ and $\tilde{z}_{t+1:t+K}$, a sequence of latent features extracted directly from the raw observations / states with $\tilde{z}_{t+k} = f_T(s_{t+k})$. For example, the self-predictive representations (SPR) [33] method utilizes a cosine similarity for prediction error, leading to the following objective:

$$\mathcal{L}_{\text{SPR}} = - \sum_{k=1}^K \left(\frac{\hat{z}_{t+k}}{\|\hat{z}_{t+k}\|_2} \right)^\top \left(\frac{\tilde{z}_{t+k}}{\|\tilde{z}_{t+k}\|_2} \right), \quad (3)$$

where \tilde{z} is often referred to as the target embedding and generated from a target encoder $f_T(\cdot)$, which is a stop-gradient version of the online encoder $f(\cdot)$.

Value Consistency. Intuitively, for a good encoder and a reasonable transition model in RL algorithms, the predictive representations should contain abundant information such that precise value estimation can be made by feeding the latent embedding into a value head. With a slight abuse of notation, we denote the Q -value predictions by a value head for the embedding-action pair (z_t, a_t) as $Q(z_t, a_t)$. For simplicity, we use $Q(z_t, \cdot)$ to denote the action values from the embedding z_t for all possible actions. In this way, the value predictions for imagined states $\hat{z}_{t+1:t+K}$ and target states $\tilde{z}_{t+1:t+K}$ can be written as $\{Q(\hat{z}_{t+k}, \cdot)\}_{k=1:K}$ and $\{Q_T(\tilde{z}_{t+k}, \cdot)\}_{k=1:K}$ respectively. Then our value-consistent representation learning loss is obtained by minimizing the distance between these two value predictions, as described by:

$$\mathcal{L}_{\text{VCR}} = \sum_{k=1}^K d_{\text{VCR}}(Q(\hat{z}_{t+k}, \cdot), Q_T(\tilde{z}_{t+k}, \cdot)), \quad (4)$$

where d_{VCR} is a distance metric for action-values to be detailed below, and $Q_{\text{T}}(\tilde{z}_{t+k}, \cdot)$ is the target value prediction generated with a target head Q_{T} . Now, we are ready to present our overall training objective as below:

$$\mathcal{L}_{\text{total}}(\theta) = \mathcal{J}(\theta) + \lambda_{\text{SPR}}\mathcal{L}_{\text{SPR}}(\theta) + \lambda_{\text{VCR}}\mathcal{L}_{\text{VCR}}(\theta), \quad (5)$$

where θ denotes all the model parameters used for computing the above loss function, and $\lambda_{\text{SPR}}, \lambda_{\text{VCR}}$ are the hyperparameters to weight different losses.

Value-Consistent Distance Metric. Here we develop our distance metric $d_{\text{VCR}}(\cdot, \cdot)$ and provide two different implementations for both discrete action and continuous settings. It seems easy to come up with an idea for $d_{\text{VCR}}(\cdot, \cdot)$. For example, one can simply apply mean-squared loss to the imagined q-values and the target q-values over all possible actions: $d_{\text{MSE}} = \sum_{a \in \mathcal{A}} [Q(\hat{z}_t, a) - Q(\tilde{z}_t, a)]^2$. Actually, this can not work through because the target action-value $Q(\tilde{z}_t, a_t)$ for the real action a_t keeps evolving as the training proceeds. Based on $\mathcal{J}(\theta)$ in Eqn. (1), at each iteration, the Q value $Q(\tilde{z}_t, a_t)$ (where $\tilde{z}_t = f(s_t)$) for a real state-action pair (s_t, a_t) will be updated towards a n -step target estimation $\bar{G}_t^{(n)}$. If we still use d_{MSE} , it means that we are optimizing $Q(\hat{z}_t, a_t)$ towards a sub-optimal point. Based on the above observation, we propose the following distance function:

$$d_{\text{VCR}} = \sum_{a \in \mathcal{A}} [Q(\hat{z}_t, a) - \bar{Q}(\tilde{z}_t, a)]^2, \quad (6)$$

$$\text{where } \bar{Q}(\tilde{z}_t, a) = \begin{cases} \bar{G}_t^{(n)} & \text{if } a = a_t, \\ Q(\tilde{z}_t, a) & \text{if } a \neq a_t. \end{cases}$$

With above equations, we let the value prediction of a real state-action pair (s_t, a_t) align with a n -step target estimation $\bar{G}_t^{(n)}$, while other pairs align with the corresponding target action-value $Q(\tilde{z}_t, a)$.

Discrete Action Implementation. For discrete actions, the Q network or head is implemented to directly generate $|\mathcal{A}|$ outputs representing the Q values for the corresponding actions. We can simply enumerate all of them to calculate the above distance in Eqn. (6). As our method is based on Rainbow, each value will be divided into several bins to build a distributional representation. The above mean-squared loss is thus replaced with a cross-entropy loss. Refer to [19] for more details.

Continuous Action Implementation. For continuous actions, the Q network has a different implementation, which usually takes both the state s_t and the action a_t and then outputs a scalar as the Q value $Q(s_t, a_t)$. In this case, we randomly sample a few actions from the policy, and then use them to calculate the distance together with the actual action a_t . Note that SAC is chosen to be our baseline algorithm, in which the target Q value is estimated by one-step return. The above $\bar{G}_t^{(n)}$ is calculated by $\bar{G}_t^{(n)} = r_t + \gamma Q_{\bar{\theta}}(s_{t+1}, a_{t+1})$. Considering soft Q values are used in SAC, we also employ soft q values when calculating the value-consistent loss. Please refer to Appendix A.1 and [14] for details.

4 Experiments

In this section, we empirically evaluate the effectiveness of our VCR on improving representation learning for RL and boosting data efficiency in low-data regimes. We then conduct ablation studies to analyze the important components in our method.

4.1 Setup

Environments. We benchmark VCR in environments where the number of interactions is limited. Specifically, we choose Atari 100K [4, 22] for discrete control tasks and DeepMind Control 100K Suite [38] for continuous suite. Atari 100K consists of 26 games, each of which allows the agent to have 100K *interaction steps* (i.e., 400K environment steps with action repeat). As for DeepMind Control 100K, following [16, 25, 40, 44], we use six environments (i.e., ball-in-cup, finger-spin, reacher-easy, cheetah-run, walker-walk, and cartpole-swingup) for benchmarking with 100K *environment steps*.

Baselines. For Atari 100K, we take SPR [33] as a *strong baseline*. Also, SimPLe [6], DER [39], OTR [23], CURL [25], DrQ [40] are chosen as baselines because all of them were state-of-the-arts in Atari 100K at their publications. EfficientZero [42], a method based on Monte-Carlo Tree Search,

Table 1: Aggregated scores achieved by different methods on Atari-100k. † denotes using virtual trajectories.

Game	SimPLe[22]	DER[39]	OTR[23]	CURL[25]	DrQ[40]	SPR[33]	VCR	PlayVirtual[44]†
IQM HNS (%)	13.0	18.3	11.7	11.3	28.0	33.7	39.7	37.4
Optimality Gap (%)	72.9	69.8	81.9	76.8	63.1	57.7	54.4	55.8

has achieved excellent performance on both Atari 100K and DeepMind Control 100K. However, considering the success comes at the cost of one order of magnitude more GPU and CPU computation complexity, we do not compare with EfficientZero here. PlayVirtual [44] is chosen as another state-of-the-art baseline, which is also a representation learning method based on SPR. For *DeepMind Control 100K*, we choose Dreamer [15], SAC+AE [41], SLAC [27], CURL [25], DrQ [40], SPR [33] and PlayVirtual [44] as our baselines. Since SPR is designed for discrete tasks, we reproduce results over 10 random seeds by a modified SPR based on SAC for continuous tasks³.

Implementation Details. For *discrete action tasks*, we base our implementation of VCR on the official code⁴ of SPR. The encoder is a three-layer convolutional network, and the transition model is a two-layer convolutional network. Q head is a two-layer linear network shared by Q -learning and Value-Consistent representation learning. For Q head, noisy parameters [11] are reserved because we verify that the noisy q-value output does not have any negative influence on Value-Consistent representation learning (see Appendix B.3). Different from SPR which has an asymmetric prediction head at the end of the online encoding branch, we validate that the removal of the prediction head would not impair the performance (see Appendix B.3). Thus we directly build q head following the encoding branch. The prediction step is set $K = 5$. Q -learning loss and Value-Consistent loss are optimized jointly by an Adam Optimizer [24], where the batch size is 32. For *continuous control tasks*, the modified SPR for continuous control is chosen as our codebase. Prediction step is set $K = 3$. Actor loss, critic loss, and Value-Consistent loss are optimized separately by three Adam optimizers [24], where the batch size for the actor-critic update is 512 and the batch size for VCR update is 128. For more details, please refer to Appendix B.1. Code will be open-sourced upon acceptance.

Evaluation Metrics. According to the recommendation [1], we choose *interquartile mean (IQM)* as *main evaluation indicator* considering its good properties. IQM trims the bottom and top 25% runs and computes the mean Human Normalized Score (HNS) of the remaining 50% runs over all games and seeds. IQM is more robust to outliers than the mean criterion. IQM is also more statistically efficient than the median value because the median only depends on one or two values. Besides, IQM has a smaller confidence interval (CI) and can detect a given improvement with far fewer runs [1]. We also report the optimality gap. *Optimality gap* denotes the gap between algorithms and the target performance. If an algorithm is evaluated on M games and N seeds, and $x_{i,j}$ denotes HNS of the i th game and the j th seed, optimality gap equals $1 - \frac{1}{MN} \sum_{i=1}^M \sum_{j=1}^N \min(x_{i,j}, \lambda)$, where λ represents the performance that algorithms aims to achieve. When all runnings reach or exceed the target performance, the optimality gap equals 0. For Atari 100K, algorithms are designed to compete with humans, so we set $\lambda = 1$. For DeepMind Control, we set $\lambda = 1,000$ as it is the highest possible score.

On Atari-100K and DeepMind Control 100K, we use 10 seeds for each game to evaluate VCR. For each run, we evaluate the agent at the end of training over N complete episodes and get the average of N scores (*i.e.*, for Atari 100K, $N = 100$; for DeepMind Control 100K, $N = 10$). As for data sources of other methods, please refer to Appendix B.2.

4.2 Results

On **Atari-100K**, as shown in Fig. 3, VCR achieves the best performance on both IQM HNS and optimality gap. It can be seen from the nonoverlapping confidence intervals that our improvement over SPR is statistically significant. Fig. 4 reveals that VCR is strictly above baselines along the whole axis, demonstrating consistent improvement over baselines. The improvement is particularly noteworthy when focusing on the HNS interval between 0.2 and 1.0. The numerical performance of methods is presented in Table 1. By adding value consistency constraint, our method gets a boost over the baseline SPR by **6.0% IQM HNS**, which is significant when considering the 5.7% IQM HNS improvement of SPR over DrQ and 3.7% of PlayVirtual over SPR. Compared to PlayVirtual,

³Link: <https://github.com/microsoft/Playvirtual>, licensed under the MIT License.

⁴Link: <https://github.com/mila-iqia/spr>, licensed under the MIT License.

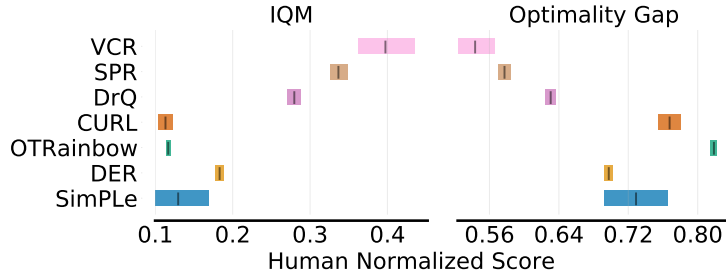


Figure 3: Aggregate IQM and optimality gap of methods. Higher IQM and lower optimality gap are better. The shaded bar shows 95% stratified bootstrap confidence intervals [1]. VCR runs 10 seeds over 26 games. The data sources of other methods can be found in Appendix B.2.

the other regularization method based on SPR architecture by producing virtual cycle trajectories, VCR achieves better performance (higher IQM HNS by 2.3%) with less computation and memory consumption (PlayVirtual needs a longer prediction step and generates ten times of trajectories. See Appendix B.1). All scores of individual games are shown in Table 4.

Table 2: Scores (mean and standard deviation) achieved by different methods on the DeepMind Control-100K. † denotes using virtual trajectories.

100k Step Scores	Dreamer[15]	SAC+AE[41]	SLAC[27]	CURL[25]	DrQ [40]	SPR[33]	VCR	PlayVirtual[44]†
Finger, spin	341 ± 70	740 ± 64	693 ± 141	767 ± 56	901 ± 104	840 ± 143	795 ± 157	683 ± 189
Cartpole, swingup	326 ± 27	311 ± 11	-	582 ± 146	759 ± 92	815 ± 48	821 ± 47	812 ± 66
Reacher, easy	314 ± 155	274 ± 14	-	538 ± 233	601 ± 213	684 ± 186	719 ± 182	663 ± 214
Cheetah, run	235 ± 137	267 ± 24	319 ± 56	299 ± 48	361 ± 67	452 ± 117	383 ± 76	510 ± 38
Walker, walk	277 ± 12	394 ± 22	361 ± 73	403 ± 24	634 ± 160	397 ± 220	650 ± 143	499 ± 161
Ball in cup, catch	246 ± 174	391 ± 82	512 ± 110	769 ± 43	914 ± 51	807 ± 165	858 ± 85	939 ± 20
IQM HNS	-	-	-	-	731	700	740	690
Optimality Gap	710	603	-	440	305	335	298	316

On **DeepMind Control 100K**, without careful finetuning of hyperparameters, VCR achieves the best performance on 3 out of 6 tasks, as shown in Table 2. In addition, VCR achieves the best IQM HNS and optimality gap. Compared with the baseline SPR, VCR has a relatively 5.7% higher IQM and 11.0% lower optimality gap.

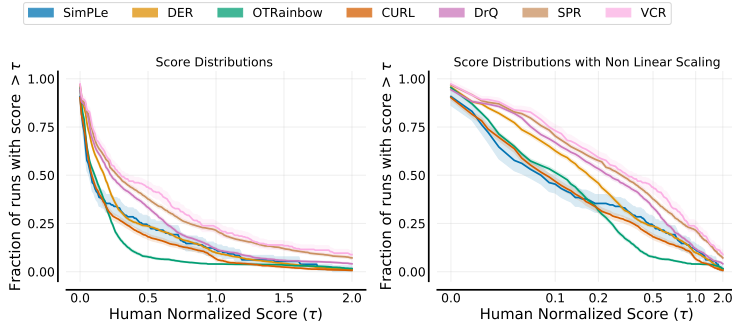


Figure 4: Performance profiles based on score distributions with linear and non-linear scaling on Atari 100K. In two plots, the y-axis represents the percentage of runs that have a score greater than the HNS τ , which the x-axis represents. The left plot shows the overall score distribution with a linear x-axis. The right plot with a scaled x-axis focuses more on the area where most runs lie. A higher curve is better. Plots are best viewed in color.

4.3 Analysis

In this section, we conduct ablation studies with Atari 100K to analyze the important components in VCR and the effectiveness of VCR compared with other auxiliary losses.

Influence of Value-Consistent Distance Metric. We find that the Value-Consistent distance metric has a great influence on the performance. We use a mixed target of n -step target estimation $\bar{G}_t^{(n)}$ and action-value $Q(\tilde{z}_t, a)$, *i.e.*, d_{VCR} (see Eqn. 6). Here, we test two variants to validate the proposed Value-Consistent distance metric. The first is to simply apply mean square loss to the imagined q -values and the target q -values over real state-action pairs: $d_{\text{MSE}} = [Q(\tilde{z}_t, a_t) - Q(\tilde{z}_t, a_t)]^2$, where \tilde{z}_t is the representation of the observation o_t . Further, we can enforce value consistency over all possible actions: $d_{\text{MSE-A}} = \sum_{a \in \mathcal{A}} [Q(\tilde{z}_t, a) - Q(\tilde{z}_t, a)]^2$.

We evaluate these two variants on Atari 100K. Note that the mean square loss is replaced with a cross-entropy for distributional RL. d_{MSE} achieves 30.9% IQM HNS and 60% optimality gap, while $d_{\text{MSE-A}}$ achieves 34.0% IQM HNS and 57.9% optimality gap. Compared to d_{VCR} (39.7% IQM HNS and 54.4% optimality gap), two variants d_{MSE} and $d_{\text{MSE-A}}$ have inferior performance. Especially for d_{MSE} , it is lower than the baseline (33.7% IQM HNS and 57.7% optimality gap). That may be because, in these two variants, VCR loss has conflicting gradients with policy learning loss (*i.e.*, DQN loss), a common issue in multi-task learning [34, 45, 21]. Q -learning loss pushes the value function towards the value distribution under the optimal policy while d_{MSE} and $d_{\text{MSE-A}}$ aim to align with the current value approximation. Intuitively, d_{MSE} has bigger conflict than $d_{\text{MSE-A}}$ because only real state-action pairs lead to an explicit conflict, which are only $1/|\mathcal{A}|$ of state-action pairs used in $d_{\text{MSE-A}}$, where $|\mathcal{A}|$ is the size of the action space. It may explain why d_{MSE} has a larger drop in performance.

Comparison with Reward Loss. One may simply attribute the improvement of VCR to the introduction of reward to representation learning in $\bar{G}_t^{(n)}$. Here, we construct a baseline by adding reward prediction based on SPR, where the dynamics model outputs predicted reward and next state conditioned on current state and action. The predicted reward is supervised by real reward. We denote this baseline as *SPR with reward loss*, which achieves 35.4% IQM HNS and 56.8% optimality gap. We see that although *SPR with reward* achieves a little higher IQM HNS than baseline, it is still far behind VCR. This implies that the effectiveness of our method should be attributed to consistent value prediction rather than involving additional reward prediction.

Comparison with Policy Learning Loss. Value-Consistent loss and policy learning loss are similar in terms of the formula form, both of which leverage Q -values to update the encoder and Q -value head. For example, in the discrete setting, both \mathcal{L}_{VCR} and \mathcal{L}_{DQN} align predicted Q -values to n -step estimation, while \mathcal{L}_{VCR} is computed over K times of state-action pairs, where K is prediction steps. Thus a possible concern is that the boost of our method comes from more state-action pairs to update the Q -value head. Here we replace \mathcal{L}_{VCR} on imagined state-action pairs with \mathcal{L}_{DQN} , equivalent to increasing the mini-batch size of \mathcal{L}_{DQN} (*i.e.*, keep batch-size of \mathcal{L}_{SPR} unchanged). We denote this modified SPR as *SPR-L* and *SPR-XL*, which separately have two and four times mini-batch size. *SPR-L* achieves 27.2% IQM HNS and 61.5% optimality gap, while *SPR-XL* achieves 17.6% IQM HNS and 70.1% optimality gap. Both two variants display performance drop, which implies VCR helps train the Q -value head but the main gain comes from its regularization on representation learning of the encoder and transition model.

Influence of Prediction Steps K . We increase the number of prediction steps from 5 to 9 to test if more improvement can be obtained. $K = 9$ achieves 39.7% IQM HNS and 54.3% optimality gap, which is roughly comparable to $K = 5$. That means increasing prediction steps in a range would not change the overall performance although the performance on a subset of games increases much (see Appendix B.3), at the cost of more computation and memory.

5 Conclusion and Limitation

To boost the sample efficiency of value-based reinforcement learning algorithms, we propose a novel *Value-Consistent Representation Learning* (VCR) method. The intuition behind VCR is that an agent should be capable of making imagination of future states from its behaviors and obtaining correct value prediction based on the imagined states. The property becomes more demanding when the environment is stochastic and learning a precise transition model is impossible. Some previous works have validated the effectiveness of this idea with policy-based methods. We develop a value-consistent metric for Q values and introduce it into value-based RL algorithms for the first time. More specifically, given a real trajectory of interactions with the environment, we employ a transition model in the latent space to shoot forward following the action sequence. Then we obtain Q -value predictions for each of the real-imagined state pairs and align them with the metric.

We further show that the method is compatible with any value-based methods by providing two implementations dealing with both discrete and continuous actions. We evaluate our method on two benchmarks including Atari 100K for discrete control and DeepMind Control 100K for continuous control. The results clearly show that VCR can improve sample efficiency significantly and achieve new state-of-the-art on both tasks. However, there are still some limitations in our method. For example, we derive the value-consistent distance metric simply employing an MSE loss, which might not be robust to value scales. We leave better distance metric investigation as future work.

References

- [1] Rishabh Agarwal, Max Schwarzer, Pablo Samuel Castro, Aaron C Courville, and Marc Bellemare. Deep reinforcement learning at the edge of the statistical precipice. *NeurIPS*, 2021.
- [2] Adrià Puigdomènech Badia, Bilal Piot, Steven Kapturowski, Pablo Sprechmann, Alex Vitvitskyi, Zhaohan Daniel Guo, and Charles Blundell. Agent57: Outperforming the Atari human benchmark. In *ICML*, 2020.
- [3] Marc G Bellemare, Will Dabney, and Rémi Munos. A distributional perspective on reinforcement learning. In *ICML*, 2017.
- [4] Marc G Bellemare, Yavar Naddaf, Joel Veness, and Michael Bowling. The arcade learning environment: An evaluation platform for general agents. *Journal of Artificial Intelligence Research*, 47:253–279, 2013.
- [5] Gino Brunner, Manuel Fritsche, Oliver Richter, and Roger Wattenhofer. Using state predictions for value regularization in curiosity driven deep reinforcement learning. In *ICTAI*, 2018.
- [6] Ting Chen, Simon Kornblith, Mohammad Norouzi, and Geoffrey Hinton. A simple framework for contrastive learning of visual representations. In *ICML*, 2020.
- [7] Xinlei Chen and Kaiming He. Exploring simple siamese representation learning. In *CVPR*, 2021.
- [8] Amir-massoud Farahmand. Iterative value-aware model learning. *NeurIPS*, 2018.
- [9] Amir-massoud Farahmand, Andre Barreto, and Daniel Nikovski. Value-aware loss function for model-based reinforcement learning. In *Artificial Intelligence and Statistics*, 2017.
- [10] Greg Farquhar, Kate Baumli, Zita Marinho, Angelos Filos, Matteo Hessel, Hado P van Hasselt, and David Silver. Self-consistent models and values. *NeurIPS*, 2021.
- [11] Meire Fortunato, Mohammad Gheshlaghi Azar, Bilal Piot, Jacob Menick, Ian Osband, Alex Graves, Vlad Mnih, Remi Munos, Demis Hassabis, Olivier Pietquin, et al. Noisy networks for exploration. In *ICLR*, 2018.
- [12] Jean-Bastien Grill, Florian Strub, Florent Altché, Corentin Tallec, Pierre Richemond, Elena Buchatskaya, Carl Doersch, Bernardo Avila Pires, Zhaohan Guo, Mohammad Gheshlaghi Azar, et al. Bootstrap your own latent—a new approach to self-supervised learning. *NeurIPS*, 2020.
- [13] Christopher Grimm, André Barreto, Satinder Singh, and David Silver. The value equivalence principle for model-based reinforcement learning. *NeurIPS*, 2020.
- [14] Tuomas Haarnoja, Aurick Zhou, Kristian Hartikainen, George Tucker, Sehoon Ha, Jie Tan, Vikash Kumar, Henry Zhu, Abhishek Gupta, Pieter Abbeel, et al. Soft actor-critic algorithms and applications. *arXiv preprint arXiv:1812.05905*, 2018.
- [15] Danijar Hafner, Timothy Lillicrap, Jimmy Ba, and Mohammad Norouzi. Dream to control: Learning behaviors by latent imagination. In *ICLR*, 2020.
- [16] Danijar Hafner, Timothy Lillicrap, Ian Fischer, Ruben Villegas, David Ha, Honglak Lee, and James Davidson. Learning latent dynamics for planning from pixels. In *ICML*, 2019.
- [17] Kaiming He, Haoqi Fan, Yuxin Wu, Saining Xie, and Ross Girshick. Momentum contrast for unsupervised visual representation learning. In *CVPR*, 2020.

- [18] Matteo Hessel, Ivo Danihelka, Fabio Viola, Arthur Guez, Simon Schmitt, Laurent Sifre, Theophane Weber, David Silver, and Hado Van Hasselt. Muesli: Combining improvements in policy optimization. In *ICML*, 2021.
- [19] Matteo Hessel, Joseph Modayil, Hado Van Hasselt, Tom Schaul, Georg Ostrovski, Will Dabney, Dan Horgan, Bilal Piot, Mohammad Azar, and David Silver. Rainbow: Combining improvements in deep reinforcement learning. In *AAAI*, 2018.
- [20] Max Jaderberg, Volodymyr Mnih, Wojciech Marian Czarnecki, Tom Schaul, Joel Z Leibo, David Silver, and Koray Kavukcuoglu. Reinforcement learning with unsupervised auxiliary tasks. In *ICLR*, 2016.
- [21] Sébastien Jean, Orhan Firat, and Melvin Johnson. Adaptive scheduling for multi-task learning. *arXiv preprint arXiv:1909.06434*, 2019.
- [22] Lukasz Kaiser, Mohammad Babaeizadeh, Piotr Miłoś, Błażej Osiniński, Roy H Campbell, Konrad Czechowski, Dumitru Erhan, Chelsea Finn, Piotr Kozakowski, Sergey Levine, Afroz Mohiuddin, Ryan Sepassi, George Tucker, and Henryk Michalewski. Model based reinforcement learning for atari. In *ICLR*, 2020.
- [23] Kacper Piotr Kielak. Do recent advancements in model-based deep reinforcement learning really improve data efficiency? 2019.
- [24] Diederik P Kingma and Jimmy Ba. Adam: A method for stochastic optimization. In *ICLR*, 2015.
- [25] Michael Laskin, Aravind Srinivas, and Pieter Abbeel. Curl: Contrastive unsupervised representations for reinforcement learning. In *ICML*, 2020.
- [26] Misha Laskin, Kimin Lee, Adam Stooke, Lerrel Pinto, Pieter Abbeel, and Aravind Srinivas. Reinforcement learning with augmented data. *NeurIPS*, 2020.
- [27] Alex X Lee, Anusha Nagabandi, Pieter Abbeel, and Sergey Levine. Stochastic latent actor-critic: Deep reinforcement learning with a latent variable model. *NeurIPS*, 2020.
- [28] Guoqing Liu, Chuheng Zhang, Li Zhao, Tao Qin, Jinhua Zhu, Jian Li, Nenghai Yu, and Tie-Yan Liu. Return-based contrastive representation learning for reinforcement learning. In *ICLR*, 2021.
- [29] Trevor McInroe, Lukas Schäfer, and Stefano V Albrecht. Learning temporally-consistent representations for data-efficient reinforcement learning. *arXiv preprint arXiv:2110.04935*, 2021.
- [30] Volodymyr Mnih, Koray Kavukcuoglu, David Silver, Andrei A Rusu, Joel Veness, Marc G Bellemare, Alex Graves, Martin Riedmiller, Andreas K Fidjeland, Georg Ostrovski, et al. Human-level control through deep reinforcement learning. *Nature*, 518(7540):529–533, 2015.
- [31] Junhyuk Oh, Satinder Singh, and Honglak Lee. Value prediction network. *NeurIPS*, 2017.
- [32] Julian Schrittwieser, Ioannis Antonoglou, Thomas Hubert, Karen Simonyan, Laurent Sifre, Simon Schmitt, Arthur Guez, Edward Lockhart, Demis Hassabis, Thore Graepel, et al. Mastering atari, go, chess and shogi by planning with a learned model. *Nature*, 588(7839):604–609, 2020.
- [33] Max Schwarzer, Ankesh Anand, Rishab Goel, R Devon Hjelm, Aaron Courville, and Philip Bachman. Data-efficient reinforcement learning with self-predictive representations. In *ICLR*, 2021.
- [34] Ozan Sener and Vladlen Koltun. Multi-task learning as multi-objective optimization. *NeurIPS*, 2018.
- [35] David Silver, Hado Hasselt, Matteo Hessel, Tom Schaul, Arthur Guez, Tim Harley, Gabriel Dulac-Arnold, David Reichert, Neil Rabinowitz, Andre Barreto, et al. The Predictron: End-to-end learning and planning. In *ICML*, 2017.

- [36] Richard S Sutton and Andrew G Barto. *Reinforcement learning: An introduction*. MIT press, 2018.
- [37] Aviv Tamar, Yi Wu, Garrett Thomas, Sergey Levine, and Pieter Abbeel. Value iteration networks. *NeurIPS*, 2016.
- [38] Yuval Tassa, Yotam Doron, Alistair Muldal, Tom Erez, Yazhe Li, Diego de Las Casas, David Budden, Abbas Abdolmaleki, Josh Merel, Andrew Lefrancq, et al. DeepMind control suite. *arXiv preprint arXiv:1801.00690*, 2018.
- [39] Hado P van Hasselt, Matteo Hessel, and John Aslanides. When to use parametric models in reinforcement learning? *NeurIPS*, 2019.
- [40] Denis Yarats, Ilya Kostrikov, and Rob Fergus. Image augmentation is all you need: Regularizing deep reinforcement learning from pixels. In *ICLR*, 2021.
- [41] Denis Yarats, Amy Zhang, Ilya Kostrikov, Brandon Amos, Joelle Pineau, and Rob Fergus. Improving sample efficiency in model-free reinforcement learning from images. *AAAI*, 2021.
- [42] Weirui Ye, Shaohuai Liu, Thanard Kurutach, Pieter Abbeel, and Yang Gao. Mastering atari games with limited data. *NeurIPS*, 2021.
- [43] Changmin Yu, Dong Li, Jianye Hao, Jun Wang, and Neil Burgess. Learning state representations via retracing in reinforcement learning. In *ICLR*, 2022.
- [44] Tao Yu, Cuiling Lan, Wenjun Zeng, Mingxiao Feng, Zhizheng Zhang, and Zhibo Chen. Playvirtual: Augmenting cycle-consistent virtual trajectories for reinforcement learning. *NeurIPS*, 2021.
- [45] Tianhe Yu, Saurabh Kumar, Abhishek Gupta, Sergey Levine, Karol Hausman, and Chelsea Finn. Gradient surgery for multi-task learning. *NeurIPS*, 2020.

Appendix

A Algorithm

A.1 Soft Actor Critic

Soft Actor Critic (SAC) [14] is a widely used off-policy algorithm for continuous control, employing policy entropy regularization as part of the reward to encourage exploration. We denote the parameters of a stochastic policy π and Q -function Q as θ and ϕ separately. SAC learns a stochastic policy π_θ , two Q -functions Q_{ϕ_1} , Q_{ϕ_2} , and a temperature weight α , which balances exploration and exploitation.

Learning Critic. To mitigate the over-estimation problem, SAC uses the double Q -networks and takes the minimal Q -value between two Q -approximators. SAC sets up the loss function for critic update over transitions (s, a, s', r, d) sampled from relay buffer:

$$\mathcal{L}_\phi^{\text{critic}} = \sum_{i=1,2} (Q_{\phi_i}(s, a) - y(r, s', d))^2, \quad (7)$$

where r is reward, s is the current state, s' is the next state, d is the terminal flag which equals 1 if s' is the terminal state, and else 0. The target is cut off gradient, given by

$$y(r, s', d) = r + \gamma(1 - d) \left(\min_{i=1,2} Q_{\phi_{\text{target},i}}(s', a') - \alpha \log \pi_\theta(a'|s') \right), \quad (8)$$

where γ is the discounted factor, $Q_{\phi_{\text{target},i}}$ is target Q -networks updated by an exponential moving average (EMA) over Q_{ϕ_i} .

Learning Actor. The actor π_θ aims to take the optimal action to maximize the action value plus the policy entropy. Thus, the actor update loss is

$$\mathcal{L}_\theta^{\text{actor}} = - \left(\min_{i=1,2} Q_{\phi_i}(s, a_\theta(s)) - \alpha \log \pi_\theta(a_\theta(s)|s) \right), \quad (9)$$

where $a_\theta(s)$ is sampled from a stochastic policy $\pi_\theta(s)$.

A.2 Pseudo Code

Here we give the pseudo code Algo. 1 for Value-Consistent representation learning, which can be easily integrated into value-based algorithms. For simplicity, the pseudo code ignores many details.

B Experiment

B.1 Training Details

Network Architecture. For discrete action tasks, the encoder is a three-layer convolutional network with (32, 64, 64) channels, (8,4,3) filter size and (4,2,1) strides. State embedding and action are concatenated together along the channel dimension as the input to the transition model, which is a two-layer convolutional network with 64, 64 channels. Q -head is a two-layer linear network shared by Q -learning and Value-Consistent representation learning with hidden unit size 256. Noisy parameters, dueling network, and double Q are utilized in Q head. Following SPR [33], the first layer of Q head is reused as projection head for SPR loss with noisy parameters and dueling network turned off. A prediction head is leveraged to calculate SPR loss, but not used for VCR loss. The target encoder f_T and target Q -head Q_T are the copy of encoder f and Q -head Q with stopping gradient.

For continuous control tasks, following CURL [25], SPR [33] and PlayVirtual [44], the encoder is a neural network with four convolutional layers and one linear layer, which outputs a 50-dimension hidden vector. The transition model is a two-layer linear network, and the first linear layer is followed by a layer normalization. Projection head and prediction head for SPR loss are built by two linear layers with 1,024 hidden units. Actor and critic are both built as a three-layer linear network, which takes as input the embedding states that the encoder produces. Exponential moving average (EMA) is employed to update the target encoder and target critic.

Loss Optimization. We split the VCR loss in Eqn. 6 into two parts. When $a = a_t$, we denote the loss of this part as $\mathcal{L}_{\text{VCR1}}$, otherwise denote as $\mathcal{L}_{\text{VCR2}}$. We denote the weight of $\mathcal{L}_{\text{VCR1}}$ as λ_{VCR} .

Algorithm 1: Value-Consistent Representation Learning

Denote parameters of the convolutional encoder f , transition model h , value head Q as θ ;
Denote parameters of the target encoder f_T , target value head Q_T as θ_T ;
Denote prediction step as K , VCR batch size as N ;
Denote Q value loss as L , Denote image augmentation as transform;
Input: a minibatch of sequences of $(s_0, a_0, r_0, \dots, s_K, a_K, r_K)$ sampled from replay buffer \mathcal{D} ;

```
for  $k$  in  $(1, \dots, K)$  do  
   $s_k \leftarrow \text{transform}(s_k)$ ; // Augment the input image batch  
end  
 $\hat{z}_0 \leftarrow f(s_0)$ ;  
 $l \leftarrow 0$ ;  
for  $k$  in  $(1, \dots, K)$  do  
   $\hat{z}_k \leftarrow h(\hat{z}_{k-1}, a_{k-1})$ ;  
   $\tilde{z}_k \leftarrow f_T(s_k)$ ;  
   $\mathcal{L}_{\text{SPR}} = - \left( \frac{\hat{z}_k}{\|\hat{z}_k\|_2} \right)^\top \left( \frac{\tilde{z}_k}{\|\tilde{z}_k\|_2} \right)$ ;  
  sample an action set  $\mathcal{A}$  that do not include  $a_k$ ;  
  calculate  $\bar{G}_k^{(n)}$  according to the specific RL algorithm;  
   $\mathcal{L}_{\text{VCR}} \leftarrow L(Q(\hat{z}_k, a_k), \bar{G}_k^{(n)})$ ; //  $\mathcal{L}_{\text{VCR}}$  for real action  
  for  $a$  in  $\mathcal{A}$  do  
     $\mathcal{L}_{\text{VCR}} \leftarrow \mathcal{L}_{\text{VCR}} + L(Q(\hat{z}_k, a), Q_T(\tilde{z}_k, a))$ ; //  $\mathcal{L}_{\text{VCR}}$  for other possible  
    actions  
  end  
   $l \leftarrow l + \lambda_{\text{SPR}} \mathcal{L}_{\text{SPR}} + \lambda_{\text{VCR}} \mathcal{L}_{\text{VCR}}$ ;  
end  
 $\theta \leftarrow \text{optimize}(\theta, l)$ ;  
update  $\theta_T$  by exponential moving average of  $\theta$ ;
```

Empirically, $\mathcal{L}_{\text{VCR}2}$ brings relatively smaller boost to performance, so a smaller weight for $\mathcal{L}_{\text{VCR}2}$ is chosen (e.g. one-tenth of λ_{VCR}). For discrete control tasks, $\lambda_{\text{VCR}} = 0.2$ is chosen for \mathcal{L}_{VCR} . Both \mathcal{L}_{VCR} and \mathcal{L}_{DQN} are cross entropy loss between two Q -value distributions. All losses are optimized jointly by an Adam optimizer. For continuous control tasks, \mathcal{L}_{VCR} is MSE loss between two Q -value scalars. $\lambda_{\text{VCR}} = 1.0$ is set. Actor loss, critic loss, temperature weight α , and VCR loss are optimized separately by four optimizers. For both discrete and continuous control, we utilize SPR loss and a warmup for λ_{VCR} to help stabilize the training of the dynamics model at the early stage of training. Following [44], a Gaussian ramp-up curve is used to increase λ_{VCR} from 0 to the maximum at the first 50K steps, and then we keep the maximum until the end of training. A full list of hyperparameters is provided in Table 9 and Table 10.

Time Complexity. Since the Value-Consistent representation learning module is disabled during collecting trajectories, the inference time of VCR is as much as SPR and PlayVirtual. We measure the time cost for training VCR, SPR, and PlayVirtual in a cluster node with one NVIDIA A100 GPU and 16 CPU cores. Prediction step is set for the best performance. Specifically, on Atari 100K, $K = 5$ for SPR and VCR, $K = 9$ for PlayVirtual; on DeepMind Control 100K, $K = 3$ for VCR, $K = 6$ for SPR and PlayVirtual. The average training time of different environments is demonstrated in Table 3. We can see when prediction step is identical on Atari 100K, VCR only takes 0.8 hour more than SPR. On DeepMind Control 100K, VCR takes nearly 46% less time because of smaller prediction step for the best setting. Additionally, we find that when prediction step is set to 3, SPR takes 2.6 hours on DeepMind Control 100K, showing VCR increases little training time (i.e. 0.5 hour). When compared with PlayVirtual, which produces tenfold virtual trajectories and takes a longer prediction step, VCR is more friendly to computation resource.

Table 3: Training time of baselines and VCR

	SPR	PlayVirtual	VCR
Atari 100K	5.6h	9.1h	6.4h
DMControl 100K	5.7h	7.3h	3.1h

B.2 Data Sources

Atari 100K. For SimPLe [22], we use their reported results of 5 seeds. Note that for DER, OTR, CURL, DrQ, and SPR, we do not use the results from the original papers [39, 23, 25, 40, 33], where results are produced by averaging 5 or 10 seeds. Instead, we report the more reliable results from [1] which run methods with 100 random seeds. The data can be found in a public cloud bucket at https://console.cloud.google.com/storage/browser/rl-benchmark-data/atari_100k. For PlayVirtual [44], we use individual runs of 15 seeds provided by the authors. We run our VCR with 10 random seeds.

DeepMind Control 100K. For Dreamer, SAC+AE, SLAC and DrQ, we use results from their papers [15, 27, 40, 41]. To compare IQM HNS and optimality gap with SPR and PlayVirtual, we rerun their codes with 10 random seeds to get score distributions. We run our VCR with 10 random seeds.

Table 4: Scores achieved by different methods on Atari-100K. † denotes using virtual trajectories.

Game	Human	Random	SimPLe[22]	DER[39]	OTR[23]	CURL[25]	DrQ[40]	SPR[33]	VCR	PlayVirtual[44]†
Alien	7127.7	227.8	616.9	802.3	570.8	711.0	865.2	841.9	822.4	947.8
Amidar	1719.5	5.8	74.2	125.9	77.7	113.7	137.8	179.7	170.6	165.3
Assault	742.0	222.4	527.2	561.5	330.9	500.9	579.6	565.6	571.6	702.3
Asterix	8503.3	210.0	1128.3	535.4	334.7	567.2	763.6	962.5	1071.5	933.3
Bank Heist	753.1	14.2	34.2	185.5	55.0	65.3	232.9	345.4	303.7	245.9
Battle Zone	37187.5	2360.0	4031.2	8977.0	5139.4	8997.8	10165.3	14834.1	13261.0	13260.0
Boxing	12.1	0.1	7.8	-0.3	1.6	0.9	9.0	35.7	42.5	38.3
Breakout	30.5	1.7	16.4	9.2	8.1	2.6	19.8	19.6	18.4	20.6
Chopper Command	7387.8	811.0	979.4	925.9	813.3	783.5	844.6	946.3	1024.2	922.4
Crazy Climber	35829.4	10780.5	62583.6	34508.6	14999.3	9154.4	21539.0	36700.5	40048.4	23176.7
Demon Attack	1971.0	152.1	208.1	627.6	681.6	646.5	1321.6	517.6	560.4	1131.7
Freeway	29.6	0.0	16.7	20.9	11.5	28.3	20.3	19.3	18.7	16.1
Frostbite	4334.7	65.2	236.8	871.0	224.9	1226.5	1014.2	1170.7	2294.7	1984.7
Gopher	2412.5	257.6	596.8	467.0	539.4	400.9	621.6	660.6	539.7	684.3
Hero	30826.4	1027.0	2656.6	6226.0	5956.5	4987.7	4167.9	5858.6	5838.8	8597.5
Jamesbond	302.8	29.0	100.5	275.7	88.0	331.0	349.1	366.5	382.5	394.7
Kangaroo	3035.0	52.0	51.3	581.7	348.5	740.2	1088.4	3617.4	3393.1	2384.7
Krull	2665.5	1598.0	2204.8	3256.9	3655.9	3049.2	4402.1	3681.6	4199.2	3880.7
Kung Fu Master	22736.3	258.5	14862.5	6580.1	6659.6	8155.6	11467.4	14783.2	19679.7	14259.0
Ms Pacman	6951.6	307.3	1480.0	1187.4	908.0	1064.0	1218.1	1318.4	1477.0	1335.4
Pong	14.6	-20.7	12.8	-9.7	-2.5	-18.5	-9.1	-5.4	0.9	-3.0
Private Eye	69571.3	24.9	34.9	72.8	59.6	81.9	3.5	86.0	98.9	93.9
Qbert	13455.0	163.9	1288.8	1773.5	552.5	727.0	1810.7	866.3	791.1	3620.1
Road Runner	7845.0	11.5	5640.6	11843.4	2606.4	5006.1	11211.4	12213.1	10746.1	13534.0
Seaquest	42054.7	68.4	683.3	304.6	272.9	315.2	352.3	558.1	521.2	527.7
Up N Down	11693.2	533.4	3350.3	3075.0	2331.7	2646.4	4324.5	10859.2	14674.1	10225.2

B.3 More Results

Full results on Atari-100K. In Table 4, we provide the performance of baselines and VCR on individual games. VCR achieves the best on 6 out of 26 games. For details of data sources, please refer to Appendix B.2.

Influence of increasing prediction step. When increasing prediction step K from 5 to 9, the overall performance of VCR is nearly unchanged. However, as Table 5 shows, larger prediction step has greater influence on scores of a subset of games. For example, Breakout, Demon Attack, and Qbert acquire at least 50% boost. However, Bank Heist, Crazy Climber, and Boxing suffer significant performance drop. This reveals that a longer prediction step can be applied to some specific environments to get better scores.

Table 5: VCR performance on Atari 100K when prediction step K is set to 5 and 9.

Game	VCR-K5	VCR-K9	Game	VCR-K5	VCR-K9	Game	VCR-K5	VCR-K9
Alien	822.4	913.7	Crazy Climber	40048.4	23218.2	Kung Fu Master	19679.7	13229.0
Amidar	170.6	160.9	Demon Attack	560.4	1178.9	Ms Pacman	1477.0	1269.1
Assault	571.6	712.7	Freeway	18.7	21.7	Pong	0.9	-3.0
Asterix	1071.5	939.6	Frostbite	2294.7	1897.0	Private Eye	98.9	100.0
Bank Heist	303.7	190.8	Gopher	539.7	656.9	Qbert	791.1	3376.1
Battle Zone	13261.0	12357.0	Hero	5838.8	7340.4	Road Runner	10746.1	12017.9
Boxing	42.5	24.2	Jamesbond	382.5	379.8	Seaquest	521.2	526.7
Breakout	18.4	27.7	Kangaroo	3393.1	3829.7	Up N Down	14674.1	11230.2
Chopper Command	1024.2	1039.5	Krull	4199.2	3987.0			

Influence of weight λ_{VCR} . We conduct experiments to study the influence of λ_{VCR} . Results in Table 6 show that the optimal setting is $\lambda_{VCR} = 0.2$ for Atari while $\lambda_{VCR} = 1.0$ for DeepMind

Control. This may be because on Atari 100K the distributional value is used, which provides stronger supervision than a scalar. So a smaller weight would be better.

Table 6: The influence of weight λ_{VCR} on VCR.

		$\lambda_{\text{VCR}} = 0$	$\lambda_{\text{VCR}} = 0.2$	$\lambda_{\text{VCR}} = 1.0$
Atari 100k	IQM HNS	33.7	39.7	28.8
	optimality gap	57.7	54.4	61.3
DMControl 100K	IQM HNS	700	707	740
	optimality gap	335	324	298

Removal of the prediction head. In contrastive learning, prediction head, which only follows the online branch, introduces asymmetry into the network architecture to avoid collapsed solutions [12]. But the prediction head collides with Value-Consistent representation learning because the prediction head would project q -value into a latent space that does not represent RL semantics. Here we verify that removing prediction head in SPR would not impair the performance. Specifically, based on the SPR code, we simply remove the prediction head and calculate SPR loss directly on the output of the projection head. We randomly choose three games in Atari 100K and run them with 10 seeds. HNS is shown in Table 7. Considering acceptable variance, removal of the prediction head has no impact on SPR performance. It may be because the contrastive learning framework in RL setting incorporates a dynamics model, which already causes asymmetry between the online and target branch. The conclusion provides a good basis for directly constructing VCR loss on q -value without a prediction head.

Table 7: The influence of removing prediction head on SPR.

	Crazy Climber	Pong	Battle Zone
SPR	1.04	0.43	0.36
SPR no prediction head	0.81	0.49	0.35

Influence of Noisy Net. Rainbow DQN employs Noisy Net [11] to encourage state-conditional exploration instead of ϵ -greedy exploration. When VCR shares Q -head with Rainbow DQN, intuitively noisy net may cause a disadvantage to Value-Consistent representation learning which aims to align two distributions of action values. Here we test the influence of noisy net on VCR. Specifically, we train a modified VCR implementation on 4 randomly chosen games with 10 seeds. The modified VCR turns off noisy layers (*i.e.* only using parameters that represent mean) when calculating VCR loss, but turns on noisy layers when calculating DQN loss. As Table 8 shows, removing noisy net for VCR loss does not boost the performance of the VCR algorithm. So it is reasonable to share noisy Q -head between DQN and VCR. It also reveals VCR’s robustness when some noise is added to values.

Table 8: The influence of NoisyNet on VCR.

	Crazy Climber	Pong	Battle Zone	Demon Attack
VCR	1.24	0.61	0.31	0.21
VCR no noise	0.85	0.61	0.28	0.26

C Potential Negative Societal Impact

In the paper, we develop a representation learning method that aims to accelerate the training of agents with fewer interaction steps. From this perspective, any negative societal impact that our method may cause is similar to that of general RL algorithms. We advocate that RL-based robotics systems, game AI and other applications should follow fair and safe principles.

Table 9: Hyperparameters for Atari. VCR -specific hyperparameters are placed in a separate column.

Hyperparameter	Setting
Gray-scaling	True
Frame stack	4
Observation downsampling	(84, 84)
Augmentation	Random shift & intensity
Action repeat	4
Training steps	100K
Max frames per episode	108K
Evaluation trajectories	100
Reply buffer size	100K
Minimum replay size for sampling	2000
Mini-batch size	32
Optimizer	Adam
Optimizer: learning rate	0.0001
Max gradient norm	10
Discount factor	0.99
Reward clipping	[-1, 1]
Double Q	True
Dueling	True
Support of Q-distribution	51 bins
Priority exponent	0.5
Priority correction	0.4 \rightarrow 1
Exploration	Noisy Net
Noisy nets parameter	0.5
Multi-step return length	10
Replay period every	1 step
Number of updates per step	2
Target Q network update period	1
EMA coefficient for target encoder	0
Prediction step K	5
λ_{SPR}	1.0
warmup of λ_{VCR}	True
λ_{VCR}	0.2

Table 10: Hyperparameters for DMControl.

Hyperparameter	Setting
Frame stack	3
Observation downsampling	(84, 84)
Augmentation	Random crop & intensity
Initial exploration steps	1000
Action repeat	2 finger-spin and walker-walk; 8 cartpole-swingup; 4 otherwise
Evaluation trajectories	10
Replay buffer size	100K
Discount factor	0.99
Initial temperature	0.1
SAC batch size	512
Actor update freq	2
EMA coefficient for target critic	0.01
Critic target update freq	2
EMA coefficient for target encoder	0.05
Prediction step K	3
λ_{SPR}	1.0
Actor opt & Critic opt & Encoder opt	
Optimizer type	Adam
(β_1, β_2)	(0.9, 0.999)
Learning rate	0.0002 cheetah-run 0.001 otherwise
Temperature (α) opt	
Optimizer type	Adam
(β_1, β_2)	(0.5, 0.999)
Learning rate	0.001
VCR batch size	128
warmup of λ_{VCR}	True
λ_{VCR}	1.0